Microphase-separated poly(styrene-*b*-isoprene)$_n$ multiblock copolymers with constant block lengths*

S. D. Smith, R. J. Spontak†‡, M. M. Satkowski, A. Ashraf, A. K. Heape and J. S. Lin§

Corporate Research Division, The Procter and Gamble Company, Cincinnati, OH 45239, USA
‡ Department of Materials Science and Engineering, North Carolina State University, Raleigh, NC 27695, USA
§ Solid State Division, Oak Ridge National Laboratory, Oak Ridge, TN 37831, USA

Linear multiblock copolymers, like their diblock analogues, are capable of ordering into periodic microstructures when the blocks are sufficiently incompatible. In this work, a series of four linear poly(styrene-*b*-isoprene)$_n$ (SI)$_n$ ($1 \leqslant n \leqslant 4$) multiblock copolymers with nearly equal block lengths has been synthesized via living sequential anionic polymerization. All of the copolymers are microphase-separated, as discerned by transmission electron microscopy (TEM) and small-angle X-ray scattering (SAXS), and exhibit lamellar morphologies in which the microdomain periodicity decreases with n. This behaviour suggests that the middle blocks contract the microdomains along the lamellar normal. Microstructural characteristics are compared with predictions from formalisms proposed for linear multiblock copolymers and, along with conformational considerations, are used to interpret the thermal and tensile properties of the copolymers.

(Keywords: multiblock copolymer; segmented copolymer; microphase separation)

INTRODUCTION

Significant effort has been put into elucidating the morphological behaviour of AB diblock copolymers in the strong-segregation regime, i.e. when $\chi_{AB}N \gg (\chi_{AB}N)_c$. Here, χ_{AB} is the Flory–Huggins interaction parameter, $N(=N_A+N_B)$ is the total number of monomers along the backbone, and subscript c denotes the order–disorder transition (ODT)[1]. For symmetric (50/50 vol%) copolymers with $N > 10^6$, $(\chi_{AB}N)_c = 10.5 + \rho N^{-1/3}$, where ρ depends[2] on monomer length and density. This class of materials possesses the simplest block architecture, consisting of two chemically dissimilar terminal blocks connected by a single covalent bond at the junction. The bond restricts phase separation and forces the incompatible blocks to order into periodic morphologies which are analogous to those generated by small-molecule amphiphiles[3].

Triblock copolymers consist of two terminal blocks and one middle block. They order much in the same way as do diblock copolymers in the strong-segregation regime, but exhibit different weak-segregation behaviour at the ODT[4]. In the ABA architecture, the B block is anchored at both ends and, upon microphase separation, is capable of adopting either a *looped* conformation, in which the junctions lie in the same interphase (λ in the lamellar morphology illustrated in *Figure 1*), or a *bridged* conformation, in which the junctions reside in adjacent interphases. If, under specified conditions, monomer A is glassy and monomer B is elastomeric, the A microdomains serve to physically crosslink the B microdomains, which, in turn, enhances the mechanical toughness of the material. The same behaviour is not, however, observed if the endblocks are elastomeric and the midblock is glassy. Thus, the mechanical properties of triblock copolymers can depend strongly on the block sequence (ABA *versus* BAB).

Since the linear triblock architecture is asymmetric, consisting of an odd number of blocks with only one middle block, and since the resultant properties are dependent on block sequencing, it is unclear whether the role of middle-block conformation in morphology and, hence, property development can be ascertained from these materials[5]. In an effort to overcome this uncertainty, we have begun to explore the microstructural and property characteristics of well-defined linear (AB)$_n$ multiblock copolymers, wherein n denotes the number of block pairs. In this architecture, the A and B moieties *each* contribute one terminal block and $n-1$ midblocks, thereby eliminating sequence-dependent properties. Many amorphous multiblock copolymers possess randomly coupled blocks which complicate systematic conformational studies[6–11], but recent efforts[12–16] have established viable synthetic routes to perfectly alternating (AB)$_n$ copolymers. These block-symmetric materials are expected to provide tremendous insight into the role of middle-block conformations, since each of the $2(n-1)$ midblocks of an (AB)$_n$ molecule can adopt either a bridged or looped conformation. It has previously been shown[17] that an

* Presented at 'The Polymer Conference', 20–22 July 1993, University of Cambridge, UK
† To whom correspondence should be addressed

0032-3861/94/21/4527–10

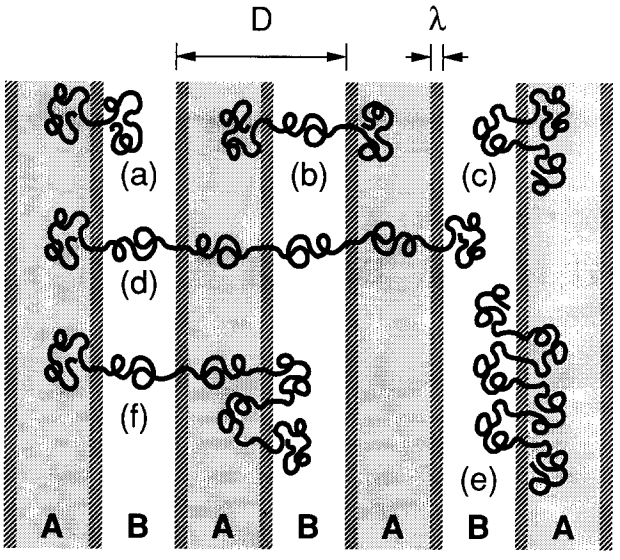

Figure 1 Schematic illustration of the molecular conformations strongly segregated linear block copolymers may adopt within the AB lamellar morphology. Only one conformation is available to the diblock copolymer (a), whereas an ABA triblock copolymer may assume two: one bridged (b) and the other looped (c). An $(AB)_3$ hexablock is capable of 16 different conformations, of which the fully bridged and fully looped limiting cases are presented in (d) and (e), respectively. An intermediate $(AB)_3$ conformation is shown in (f) for the sake of comparison. The microdomain periodicity D and interphase thickness λ are also shown

$(AB)_n$ molecule is capable of assuming $2^{2(n-1)}$ different molecular conformations, some of which are illustrated in *Figure 1*.

The objectives of the present work are three-fold: (i) ascertain the effect of the $(AB)_n$ architecture on ordered morphologies in a series of copolymers possessing nearly equal block lengths; (ii) deduce conformational preferences by comparing the data obtained here with predictions from theoretical formalisms proposed for linear multiblock copolymers; and (iii) determine the effect of molecular architecture on bulk properties by relating these molecular and microstructural characteristics to bulk thermal and tensile properties.

EXPERIMENTAL

Materials

Four multiblock copolymers composed of perfectly alternating styrene and isoprene blocks and denoted here by $(SI)'_n$ (with $1 \leqslant n \leqslant 4$) were synthesized via living sequential anionic polymerization in cyclohexane at 60°C. [The prime sign is used to differentiate these copolymers of nearly constant block length from $(SI)_n$ copolymers possessing constant molecular weight.] Sec-butyl lithium was used as the initiator, and polymerization times of 30 min for styrene and 90 min for isoprene were selected to guarantee complete monomer consumption during block formation. The protocol by which these $(SI)'_n$ copolymers were synthesized is described in detail elsewhere[14,16]. Each copolymer possessed block weights of 15 000–18 000 g mol^{-1}, as determined from g.p.c. and ^{1}H n.m.r. Chromatograms also revealed that these materials were relatively monodisperse, with $\bar{M}_w/\bar{M}_n < 1.09$. The molecular characteristics of these four copolymers are tabulated in *Table 1*.

Methods

Film production. Copolymer films were obtained by first casting 4% (w/v) toluene solutions (unless otherwise indicated) into Teflon moulds. Upon slow solvent removal over the course of 3 weeks in a solvent-rich atmosphere, resultant films measured ~3 mm thick. They were heated to 50°C at ambient pressure and 90°C under low vacuum (~0.13 Pa) for 1 day to remove excess solvent and were subsequently encapsulated in glass tubes, cycled between high vacuum and Ar three times, and sealed under an Ar atmosphere. The assemblies were annealed for 1 week at 165°C and then allowed to cool slowly (≈ -0.5°C min^{-1}) to ambient temperature. No signs of gross oxidative degradation (i.e. colour change) were visible, and the films could be redissolved in toluene.

Morphological analysis. Ultrathin specimens for transmission electron microscopy (TEM) were obtained by sectioning the thick films at −100°C with a Diatome 35° cryodiamond knife on a Reichert-Jung FC-4E ultramicrotome. The isoprene-rich microdomains were preferentially stained with the vapour of 2% aqueous OsO_4 for 90 min. Electron micrographs were obtained on a Zeiss EM902 electron spectroscopic microscope, operated at an accelerating voltage of 80 kV and an energy loss (ΔE) of 50 eV. Specimens for small-angle X-ray scattering (SAXS) were produced by cutting the bulk films into ~2–3 mm thick strips, which were then rotated 90° and mounted side-by-side. Two-dimensional scattering patterns were recorded with edge-on CuKα radiation on

Table 1 Molecular and microstructural characteristics of the multiblock copolymers examined here[a]

Designation	n	M_B ($\times 10^{-3}$) (g mol^{-1})	M ($\times 10^{-3}$)[d] (g mol^{-1})	W_S[e]	SAXS[b] D (nm)	SAXS[b] D_c[f] (nm)	TEM[c] D (nm)	TEM[c] D_c[f] (nm)
$(SI)'_1$	1	15	30	0.50	27.5	27.5	32.3	32.3
$(SI)'_2$	2	18	72	0.50	27.0	24.6	27.0	24.6
$(SI)'_3$	3	18	108	0.50	26.0	23.7	24.7	22.4
$(SI)_4$[g]	4	15	120	0.50	19.6	19.6	18.3 (20.6)	18.3

[a] M_B, M and W_S denote block weight ($=M_{AB}/2$), total molecular weight and total styrene weight fraction, respectively
[b] Experimental error of ±1 nm
[c] Estimated error of ±2 nm
[d] Determined from g.p.c.
[e] Determined from ^{1}H n.m.r.
[f] Corrected for block length
[g] Value in parentheses obtained from a chloroform-cast film

the 10 m instrument at the National Center for Small-Angle Research (Oak Ridge National Laboratory, TN). The patterns were collected for 1–4 h at 40 kV and 100 mA and were presumed to be free of smearing effects due to the pinhole collimation and sample-to-detector distance (5.18 m). Corrections were made for background scattering, absorption, detector sensitivity and dark current.

Property analysis. Small quantities (~ 10 mg) of the same films used for TEM and SAXS were also examined by differential scanning calorimetry (d.s.c.) on a Mettler model no. 30 calorimeter. Specimens were heated to 150°C within the calorimeter and then immediately cooled at a rate of -10°C min^{-1} to -100°C, after which thermograms were collected at 20°C min^{-1} from -100°C to 150°C under N_2 (to avoid degradation). Films permitted to undergo slow solvent evaporation and heated to remove residual solvent (but *not* annealed at 165°C) were cut into strips measuring 5.1 cm long and 1.3 cm wide. They were subsequently subjected to uniaxial tensile deformation at 25°C on an Instron model no. 1122 instrument, operated at crosshead speeds of 0.5 and 12.7 cm min^{-1}.

RESULTS AND DISCUSSION

Microstructural properties

Electron microscopy. *Figure 2* is a series of electron micrographs obtained from the $(SI)'_n$ copolymers, clearly demonstrating that each material exhibits the lamellar morphology, which is expected for strongly segregated symmetric copolymers. The lamellae observed in $(SI)'_1$ (*Figure 2a*) and $(SI)'_2$ (*Figure 2b*) appear indistinguishable in terms of both their thickness and periodicity (D). It must be remembered, however, that the blocks in $(SI)'_2$ are longer (by 20%, from *Table 1*) than those comprising $(SI)'_1$. Comparison of $(SI)'_3$ (*Figure 2c*) and $(SI)'_2$ (*Figure 2b*), on the other hand, reveals that the microstructural dimensions of the hexablock are noticeably smaller than those of the tetrablock (both of which consist of 18 000 g mol^{-1} blocks), while the lamellae visible in the

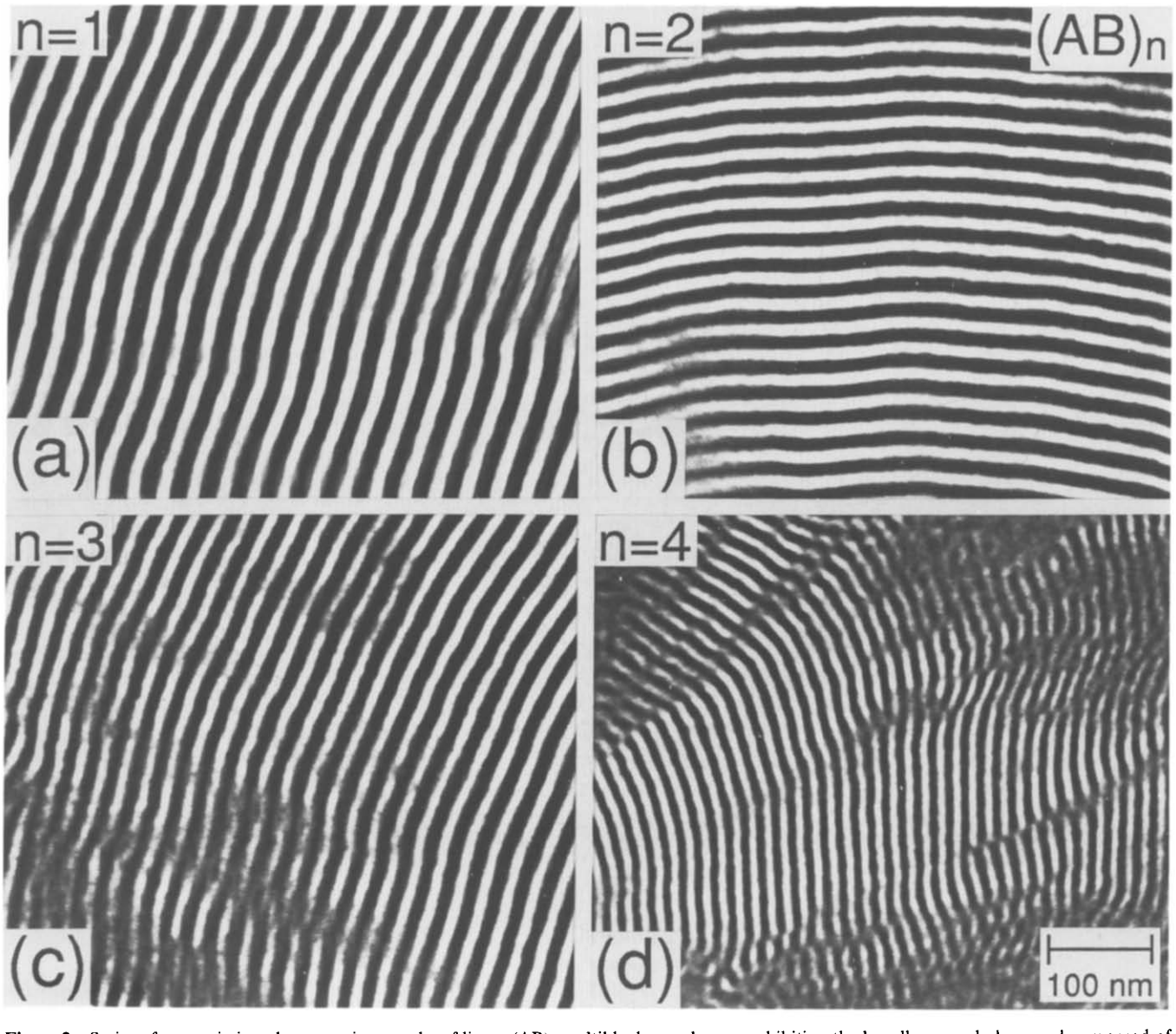

Figure 2 Series of transmission electron micrographs of linear $(AB)_n$ multiblock copolymers exhibiting the lamellar morphology and composed of styrene and isoprene blocks of nearly constant mass. Values of n are (a) 1, (b) 2, (c) 3 and (d) 4. The isoprene lamellae appear dark in these micrographs due to OsO_4 staining

$(SI)_4$ octablock copolymer* (*Figure 2d*) exhibit the smallest D of the series. This trend suggests that the microdomains contract as n is increased, an observation we address at length later. Average values of D obtained from electron micrographs such as those presented in *Figure 2* for each of the copolymers are included in *Table 1*.

The micrographs in *Figure 2* also demonstrate another trend, namely, that the grain size (G) of oriented lamellae decreases with n. Some morphological imperfections are evident in the series of images, but this reduction is not obvious in *Figures 2a–c*, since $G \gg D$. In the octablock copolymer (*Figure 2d*), however, G is on the order of D, presumably due to mobility restrictions placed upon the chains during quiescent microphase separation. Irregularly shaped grains of lamellae are evident in this micrograph, as are regions which appear disordered. From TEM micrographs obtained at different tilt angles and electron tomography[18], these regions have been found to correspond to lamellae which are not oriented normal to the electron beam. Orientational disorder induced by a reduction in G should not be confused with thermodynamic disorder, which occurs when $\chi_{AB}N < (\chi_{AB}N)_c$ and results in fluctuating assemblies which are reminiscent of coexisting A and B close-packed micelles[19–21].

An additional micrograph of the $(SI)_4$ copolymer is provided in *Figure 3*. Unlike the one displayed in *Figure 2d*, this micrograph is obtained from the copolymer after it had been dissolved in and cast from chloroform, which is a preferential solvent for polystyrene ($\delta_{CHCl_3} \approx 9.3$ H, $\delta_S \approx 9.1$ H, and $\delta_I \approx 8.1$ H, where δ is the solubility parameter). Investigations[5,22,23] into the effect of solvent quality on block copolymer morphology have shown that preferential solvents tend to either swell one microdomain or alter the ultimate morphology altogether. Very little difference in morphology is, however, evident from *Figures 2d* and *3*. In fact, the lamellar periodicity obtained from micrographs such as the one in *Figure 3* (and provided in *Table 1*) is comparable to that measured earlier for the $(SI)_4$ copolymer cast from toluene, indicating that microdomain swelling due to a preferential solvent may be less pronounced in linear multiblock copolymers ($n > 1$), which possess considerable molecular interconnectivity, than in diblock copolymers.

SAXS. Two-dimensional scattering patterns for the copolymers investigated here are shown in *Figure 4*. The one acquired from $(SI)'_1$ (*Figure 4a*) appears to be the most anisotropic, possessing well-defined meridional and equatorial arcs. As n increases in *Figures 4b–d*, though, the patterns become more isotropic, indicating a corresponding increase in the orientational distribution of scattering. This behaviour is consistent with a reduction in G with n. Intensity profiles generated by integrating these patterns have already been presented[15] and are not reproduced here. Suffice it to say that the profiles reveal several important features in the low-h regime, where scattering maxima arise from ordered morphologies. Here, h denotes the magnitude of the scattering vector and is defined by:

$$h \equiv \frac{4\pi}{\lambda_r} \sin\theta \qquad (1)$$

where λ_r is the wavelength of the CuKα radiation (0.154 nm) and θ is the scattering angle. The first feature to be addressed in this vein is the position of the principal scattering peak (h^*). SAXS profiles reveal that h^*

* The prime sign is removed from $(SI)_4$ since this copolymer is also part of the $(SI)_n$ series presented elsewhere[14,16]

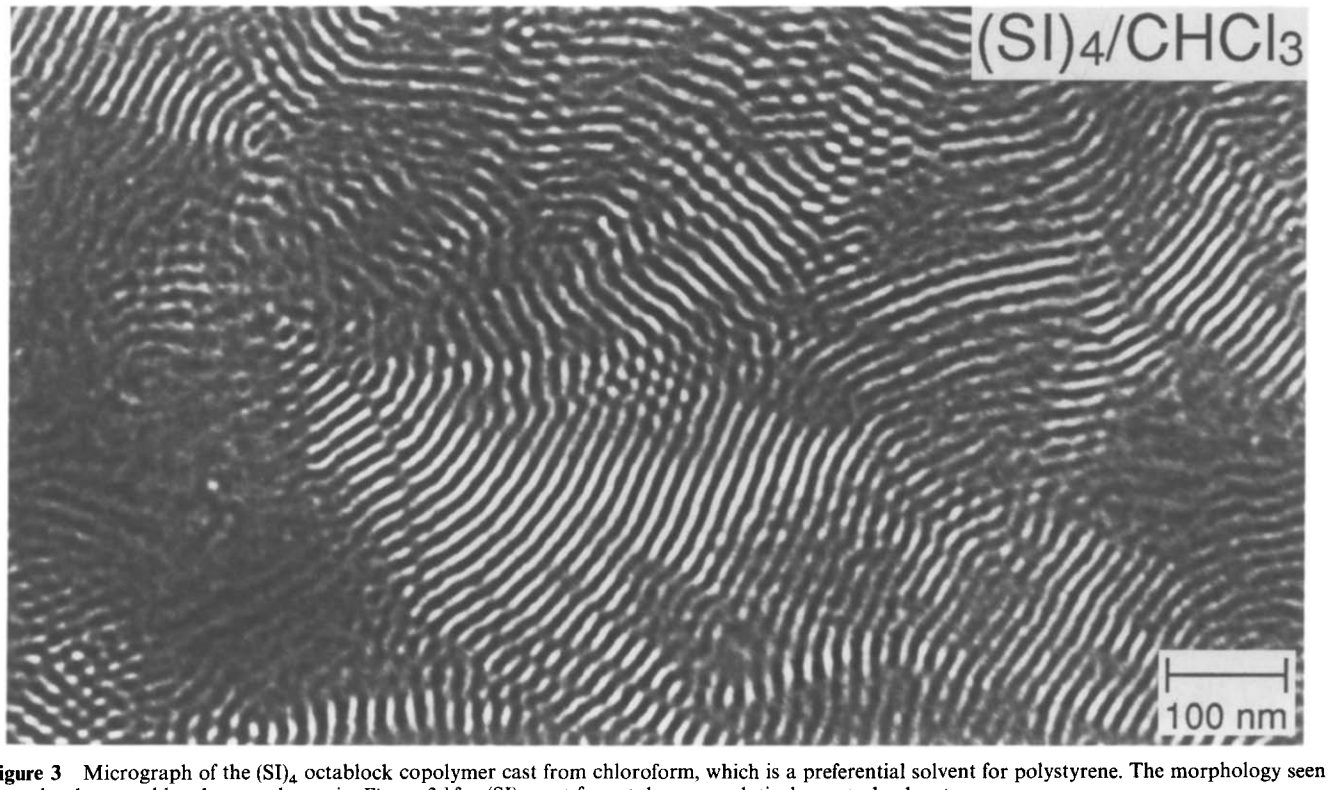

Figure 3 Micrograph of the $(SI)_4$ octablock copolymer cast from chloroform, which is a preferential solvent for polystyrene. The morphology seen here closely resembles the one shown in *Figure 2d* for $(SI)_4$ cast from toluene, a relatively neutral solvent

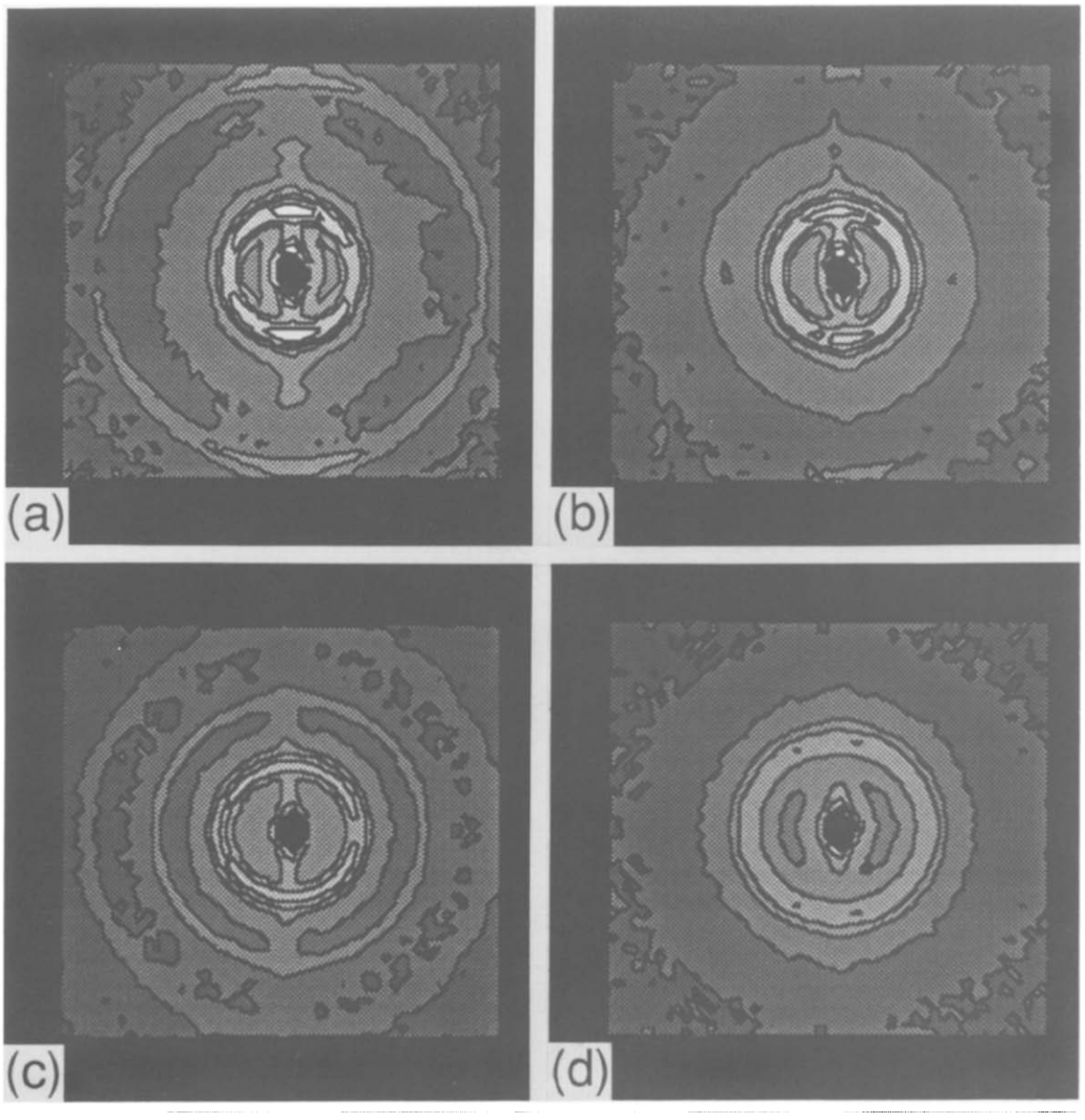

Figure 4 Two-dimensional SAXS patterns obtained from the $(AB)_n$ multiblock copolymers described in the caption of *Figure 2*. Scattering reflections arising from the microphase-separated lamellar morphology are evident. The patterns shown here become more isotropic as n increases from 1 (a) to 4 (d), suggesting that the grain size of oriented lamellae decreases with n

increases, slightly for $(SI)'_1$, $(SI)'_2$ and $(SI)'_3$, with n. Since h^* is inversely related to D via Bragg's law, $D = 2\pi/h^*$, this trend signifies that D decreases with n, in agreement with earlier observations. Values of D from SAXS are tabulated in *Table 1* and compare favourably with those ascertained from TEM.

Another salient feature of the SAXS profiles is that each copolymer exhibits a second peak at $2h^*$, implying relatively long-range order. As n increases, however, the intensity of this second peak steadily decreases, again reflecting the reduction in G discussed earlier. Methods aimed at enhancing long-range order and reducing the fraction of defects and grain boundaries in these multiblock copolymers are now under consideration, with shear-induced orientation demonstrating the most promise thus far[24,25]. Lastly, an intermediate peak between h^* and $2h^*$, indicative of compositions slightly removed from 50/50 (wt%) S/I, is also evident in the profiles from the copolymers consisting of 18 000 g mol^{-1} blocks, i.e. $(SI)'_2$ and $(SI)'_3$.

Conformational characteristics. In microphase-separated diblock and triblock copolymers, the variation of D with total molecular weight (M) has proven valuable as a means of elucidating molecular conformation. For strongly segregated diblock copolymers possessing the lamellar morphology, D is found to scale as $M^{2/3}$, which implies that the molecules assume an extended conformation along the lamellar normal[26-29]. In the present work, we are interested in determining the conformational properties of multiblock copolymers and therefore seek to examine more closely the relationship between D and n. While the copolymers investigated here possess nearly equal block lengths, the block lengths are not, in fact, equal. This complication can be alleviated by rescaling each D by the gyration radius (R_g) of the AB block pair. These corrected D, denoted D_c, are included in *Table 1*. We further elect to normalize these D_c with respect to that of the diblock copolymer to demonstrate the extent of microdomain contraction with n. Thus, a reduced periodicity (D_r) is conveniently defined

as:

$$D_r \equiv \left[\frac{D(n)}{D(n=1)}\right]\left[\frac{R_g(n=1)}{R_g(n)}\right] \quad (2)$$

Since $R_g = K_{AB}(M_{AB}/6)^{1/2}$, where K_{AB} and M_{AB} denote the Kuhn statistical length and mass, respectively, of an AB block pair, equation (2) immediately reduces to:

$$D_r = \left[\frac{D(n)}{D(n=1)}\right]\left[\frac{M_{AB}(n=1)}{M_{AB}(n)}\right]^{1/2} \quad (3)$$

Figure 5 displays the relationship between D_r and n, as discerned from both TEM and SAXS. Recall that the principal difference among these copolymers is the fraction (ξ) of double-anchored middle blocks, $\xi = (n-1)/n$. The extent to which the microdomains are contracted in *Figure 5* is therefore attributed to the presence of the middle blocks, and the functional characteristics of $D_r(n)$ in the limits of small n (where data now exist) and $n \to \infty$ (where $\xi \to 1$) are expected to provide insight into the role of middle blocks in morphological development. This topic is discussed next in the context of several theoretical formalisms which further help to identify the middle-block conformations capable of contracting the microdomains along the lamellar normal.

Krause[30] first proposed a formalism designed to address the thermodynamics of linear $(AB)_n$ multiblock copolymers. It is capable of predicting trends in the phase behaviour of these materials, but it cannot address microstructural dimensions such as D. Benoit and Hadziioannou[31] developed a theoretical framework which extends the original mean-field concepts developed by Leibler[1] for weakly segregated diblock copolymers and permits explicit prediction of D for symmetric $(AB)_n$ copolymers in the vicinity of $(\chi_{AB}N)_c$. Identical results are obtained from the theory recently proposed by Kavassalis and Whitmore[32], who applied a functional integral method[33] to both symmetric $(AB)_n$ and asymmetric $(AB)_nA$ copolymers. The predictive capabilities of both approaches have been found to be in excellent quantitative agreement. In terms of D_r, these predictions have been correlated with n to yield:

$$D_r \approx \left(\frac{\alpha-\beta}{\alpha-\beta n^{-0.86}}\right)^{1/2} \quad (4)$$

where α (= 19.3) is the limiting value of $3h^{*2}R_g^2$ as $n \to \infty$, and β (= 7.9) corresponds to the difference in $3h^{*2}R_g^2$ between $n = 1$ and $n \to \infty$[15]. Both formalisms consequently predict that D_r is bounded between 1.0 ($n = 1$) and 0.77 ($n \to \infty$). Equation (4) is plotted in *Figure 5* and is seen to agree well with the experimental data, even though the copolymers are microphase-separated.

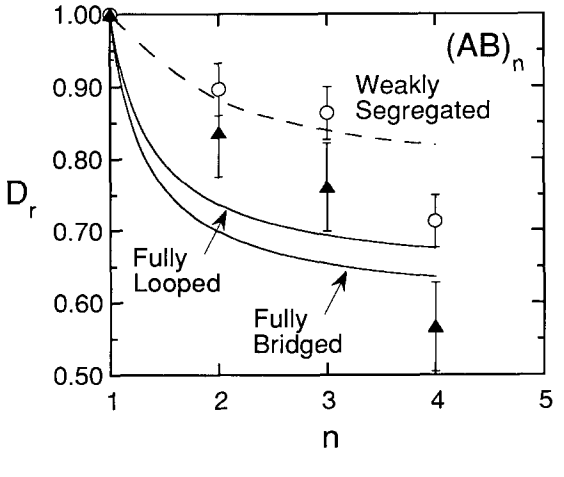

Figure 5 Lamellar periodicities for $(AB)_n$ multiblock copolymers of nearly constant block mass, reduced according to equation (3) and plotted here as a function of n. Experimental values obtained from TEM (▲) and SAXS (○) are in good agreement and indicate that the microdomains contract as n increases. Predictions from references 31 and 32 are presented as the dashed line, whereas those from equation (7) are displayed for the fully looped and bridged midblock conformations (in the strong-segregation regime) as solid lines. The vertical lines denote experimental error bars (±1 nm for SAXS and ±2 nm for TEM)

Another approach adopted to model the thermodynamics of $(AB)_n$ multiblock copolymers employs the confined single-chain statistics originally developed[34,35] for strongly segregated diblock and triblock copolymers. A detailed description of this theoretical framework is given elsewhere[17,36], but two limiting conformations warrant mention here. The first is the *fully looped* conformation, in which every middle block of an $(AB)_n$ molecule is looped so that only one λ is occupied, and the other is the *fully bridged* conformation, in which each middle block is bridged and $2n-1$ different interphases are traversed. Predictions corresponding to these limits either overestimate (fully looped conformation) or underestimate (fully bridged conformation) experimental data[15]. A symmetric $(AB)_n$ molecule ($n > 1$) exhibiting the most probable (average) conformation has been shown[17] to possess $n-1$ looped midblocks and traverse $2(n-1)^{1/2}$ different interphases. Values of D_r predicted for this conformation are in favourable agreement with experimental results, suggesting that the molecules assume the most probable conformation (i.e. partly looped and partly bridged) if permitted to order under quiescent conditions[15]. This formalism also predicts that $(AB)_n$ multiblock molecules are stretched further along the lamellar normal than their diblock counterparts.

Recent extensions of the theory developed by Semenov[37] for linear diblock copolymers to ABA triblock copolymers[38], cyclic diblock copolymers[39] and AXB triblock terpolymers[40] in the strong-segregation regime suggest that the formalism can also be applied to linear multiblock copolymers. The free-energy expressions for the terminal blocks in an $(AB)_n$ copolymer are identical to those derived for diblock molecules, but potentials accurately describing double-anchored middle blocks must account for two restricting junctions. Zhulina and Halperin[38] and Marko[39] have proposed that looped blocks are analogous to a dense brush of shortened endblocks possessing one-half the number of monomers. This presumption has recently been proven in the case of lamellar ABA triblock copolymers[41] and is currently being examined for more complex molecular architectures. If, on the other hand, the middle blocks adopt a bridged conformation, they should behave as uniformly stretched Gaussian coils[38,40].

In the narrow interphase limit[42], an approximate expression for the total free energy per unit volume ($\mathscr{F}$) of an incompressible $(AB)_n$ copolymer possessing the lamellar morphology can be written as:

$$\mathscr{F} = \frac{f}{2R_A}\left[\frac{\pi^2 R_A^3}{24nfa^2N_A^2} + \frac{\Omega(n-1)R_A^3}{nfa^2N_A^2} + 2a\chi_{AB}^{1/2}\right] \quad (5)$$

where $f (= N_A/N)$ is the fraction of monomer A, a is the

monomer gyration radius, and R_A is the half-width of an A-lamella. The coefficient Ω assumes different numerical values for looped ($\Omega = \pi^2/6$) and bridged ($\Omega = 2$) midblock conformations. The periodicity at equilibrium is obtained through minimization of equation (5) with respect to R_A, followed by substitution of D for R_A ($D = 2R_A/f$), so that:

$$D = \frac{4}{\sqrt{6}}\left(\frac{3}{\pi^2}\right)^{1/3} bN^{2/3}\chi_{AB}^{1/6}\left[\frac{n}{1+\Lambda(n-1)}\right]^{1/3} \quad (6)$$

where b denotes monomer segment length and $\Lambda = 24\Omega/\pi^2$. Normalizing equation (6) with respect to D evaluated at $n = 1$ yields the corresponding expression for D_r, namely:

$$D_r = \left[\frac{n}{1+\Lambda(n-1)}\right]^{1/3} \quad (7)$$

In the limit as $n \to \infty$, this relationship for $D_r(n)$ approaches 0.63 for non-uniformly stretched (looped) midblocks or 0.59 for uniformly stretched (bridged) midblocks, both of which are less than the limiting value obtained earlier (0.77). Equation (7) is plotted in *Figure 5* for comparison not only with the TEM and SAXS data, but also with predictions from the weak-segregation formalism previously discussed. Predictions based on equation (7) do not agree very well with the data in general, suggesting that either the copolymers examined here do not reside within the strong-segregation regime, or that the assumptions made in deriving equation (5) fail to properly account for the block conformations and block junction population ($2n-1$ block junctions/molecule) in linear multiblock copolymers.

A caveat that must be considered when microstructural characteristics (e.g. D) are compared, especially on a quantitative basis, with theoretical predictions is the requirement for equilibrium. Whether thermodynamic equilibrium can ever be truly achieved in $(AB)_n$ multiblock copolymers remains questionable due to the constraints placed on block mobility during microphase separation. In the present work, we have sought to provide the copolymers with reasonable opportunity to attain preferred molecular conformations and, hence, equilibrium under quiescent conditions. Even with such precautions, though, the formation of metastable conformations and morphologies remains a viable possibility.

Macroscopic properties

Thermal analysis. Thermograms obtained from slowly dried and annealed samples of the multiblock copolymers are presented in *Figure 6*. Two increasing step functions, each representative of a glass transition temperature (T_g), are clearly visible in every trace and correspond to the isoprene block (T_g^I) in the vicinity* of $-60°C$ and the styrene block (T_g^S) at temperatures above 70°C. The existence of block-specific T_gs is indicative of phase demixing and therefore constitutes a fingerprint of microphase separation. Several interesting characteristics regarding the dependence of these T_gs on n are evident from *Figure 6*. For instance, the T_g^I are virtually independent of n, varying by no more than $\pm 2°C$ (which is within experimental error), when $n < 4$. In the case of the octablock copolymer, though, the T_g^I is found to increase to $\sim -50°C$, which is presumed to correspond to enhanced phase mixing (discussed below). The T_g^S

* The isoprene blocks possess 94–95% of the 1,4-*cis* configuration; the T_g of 1,4-*cis* polyisoprene is $\sim -72°C$

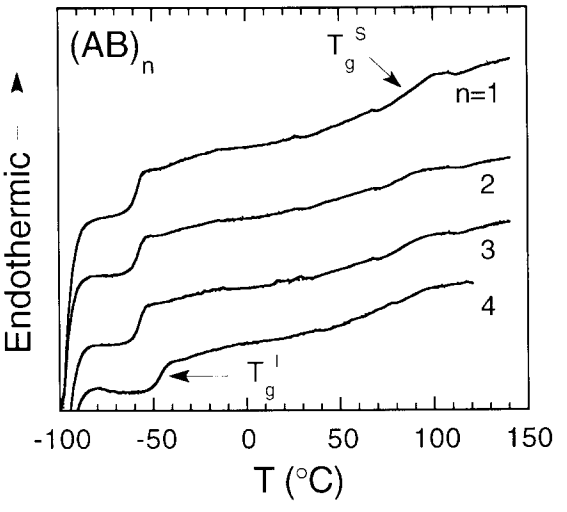

Figure 6 D.s.c. thermograms obtained from the $(AB)_n$ copolymers, illustrating the dependence of the upper (styrene) and lower (isoprene) glass transition temperatures (T_g^S and T_g^I, respectively) on n. The heating rate was 20°C min^{-1}, and the experiments were conducted under N_2 to minimize specimen degradation at elevated temperatures. Note that the T_g^I are virtually independent of n when $n < 4$

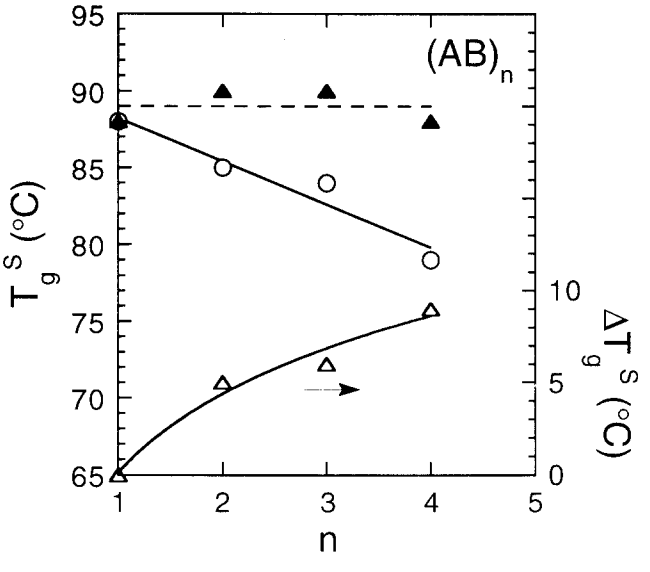

Figure 7 Dependence of T_g^S on n in linear $(AB)_n$ multiblock copolymers of nearly constant block mass. Experimental points (○) are obtained from the thermograms shown in *Figure 6*, and the predicted[44] T_g^S for polystyrene homopolymers of equal block mass are also shown (▲). The difference between the predicted and experimental T_g^S values is attributed to interphase mixing[45] and is denoted in the figure by ΔT_g^S (△). Solid and dashed lines are drawn here as guides for the eye

values, on the other hand, are much broader than the T_g^I and appear to decrease continuously with n. To more clearly demonstrate this apparent trend, they are displayed as a function of n in *Figure 7*. Since the styrene blocks are all approximately the same length and since the T_g^I do not vary much with n (especially when $n < 4$), the $T_g^S(n)$ relationship observed in *Figure 7* reveals two important microstructural ramifications: (i) the fraction of phase-mixed material increases with n, and (ii) this fraction becomes increasingly rich in polystyrene.

As microphase separation occurs upon cooling from a homogeneous melt or upon solvent removal from solution, A and B monomer segments connected to a shared block junction cannot segregate and consequently remain mixed within an interphase (λ). In the case of a

styrene block, the restricted segment residing within an interphase has been found[43] to remain relatively mobile, while the remainder of the block, safely removed from the junction, is capable of vitrifying, as would its parent homopolymer at a T_g that is dependent on sequence length. Glass transition temperatures of homopolystyrene (hPS) possessing molecular weights of 15000 and 18000 g mol^{-1} can be accurately estimated from the correlation proposed by Lu and Jiang[44]:

$$T_g^S = \frac{2N_S T_g^{S,\infty}}{2N_S + C_S^\infty f(y)} \quad (8)$$

where N_S is the number of styrene monomers, $T_g^{S,\infty} = 373$ K, $C_S^\infty = 10.68$, and $f(y)$ is determined from the worm-like chain model:

$$f(y) = 1 - 3y + 6y^2 - 6y^3(1 - e^{-1/y}) \quad (9)$$

For a vinyl polymer chain, $y = C_S^\infty/[4N_S \sin^2(54.75°)]$. Predictions from equation (8) are included in *Figure 7* and exceed the T_g^S values recorded from the multiblock copolymers. The depression in T_g^S, denoted here by ΔT_g^S [$= T_g^S$(theory) $- T_g^S$(exp.)] and also plotted in *Figure 7*, can most likely, then, be attributed to interphase mixing[45].

Enhanced phase mixing induced by molecular architecture (in this case, n) is consistent with the morphological characteristics presented earlier. The volume fraction of interphase material (f_λ) is equal to $2\lambda/D$ in the lamellar morphology. If λ is assumed, for the sake of illustration, to be independent of n (although separate studies[16] indicate that λ increases rather abruptly with n), the decrease in $D(n)$ shown in *Figure 5* also results in an increase in f_λ with n. Thus, microstructural and bulk properties both reveal that the fraction of phase-mixed material in these multiblock copolymers increases, and the driving force favouring microphase separation decreases, with n. Results from d.s.c. also demonstrate that, due to the relative invariance of $T_g^1(n)$, this fraction becomes increasingly rich in styrene, thereby supporting the concept of an asymmetric interphase composition profile in ordered block copolymers[46–48].

Mechanical analysis. Representative tensile stress–strain (σ–ε) curves for the $(SI)'_2$, $(SI)'_3$ and $(SI)_4$ copolymers drawn at a speed of 0.5 cm min^{-1} are shown in *Figure 8*. Here, the engineering stress (draw force/initial specimen area) is shown for elongations up to 30%. The diblock copolymer $(SI)'_1$ is not included since it readily failed when placed between the grips of the Instron. A yield point (i.e. a peak in the σ–ε curve, usually at low ε) and a subsequent plastic flow regime are both clearly evident for each curve in *Figure 8*. As n increases, the magnitude of the yield point is observed to increase, as are the drawing stress and stress drop upon yielding. While no specimens were elongated to break (to determine the fracture strength or energy), an increase in the relative area under the σ–ε curves with n signifies a corresponding increase in copolymer toughness. Qualitatively similar results (not shown here) have been obtained at faster crosshead speeds (e.g. 12.7 cm min^{-1}), and elongations of at least 300% have been recorded without any evidence of failure.

Graphical representations of the yield stress (σ_y), yield strain (ε_y) and Young's modulus (E) as functions of n are presented in *Figures 9–11*, respectively. Since the diblock copolymer (with 15000 g mol^{-1} blocks) could not withstand tensile deformation, it is assigned yield properties of $\sigma_y = 0$ and $\varepsilon_y = 0$ in *Figures 9* and *10*. *Figure 9* shows that σ_y increases with n at crosshead speeds of both 0.5 and 12.7 cm min^{-1}. This behaviour can be interpreted in terms of architecture-enhanced microstructural interconnectivity[49]. As the number of blocks ($2n$) increases in this copolymer series, adjacent microdomains become increasingly more connected by single molecules. Recall that an $(AB)_n$ molecule (with $n > 1$) adopting the most probable conformation in the lamellar morphology traverses $2(n-1)^{1/2}$ different interphases. This means that a poly(styrene-*b*-isoprene)$_n$ molecule on average resides in $(n-1)^{1/2}$ glassy polystyrene microdomains, with each serving as a physical crosslink at ambient temperature. As anticipated, the rigidifying effect of these crosslinks is seen (*Figure 9*) to be more pronounced at fast rates of copolymer deformation. Since similar $\sigma_y(n)$ behaviour has also been observed[16] in $(SI)_n$

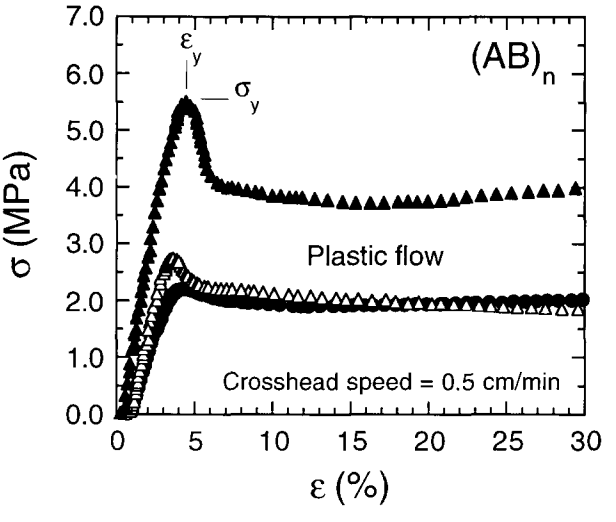

Figure 8 Tensile stress–strain curves recorded at a crosshead speed of 0.5 cm min^{-1} for the $(AB)_n$ copolymers with the following n: 2 (●), 3 (△) and 4 (▲). The diblock copolymer ($n = 1$) is not included since it readily failed. Yield points, showing both σ_y and ε_y in the case of $n = 4$, and plastic-flow regimes are clearly evident in each curve. These studies were all conducted at 25°C

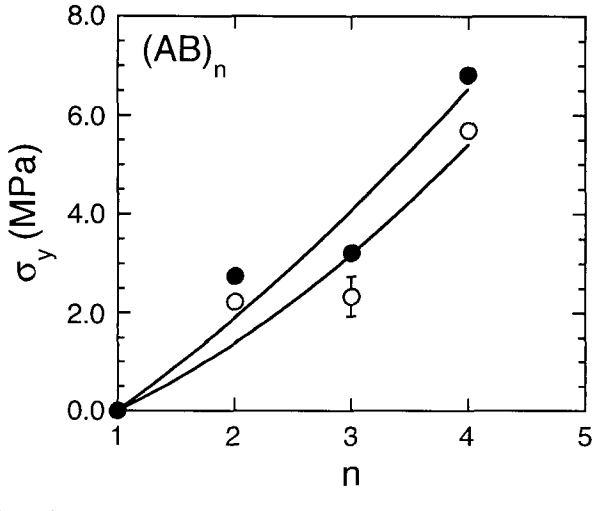

Figure 9 Dependence of the mean yield stress (σ_y) on n, discerned from curves such as those seen in *Figure 8*. Here, σ_y is observed to increase with the number of block pairs (n) at two different drawing speeds: 0.5 (○) and 12.7 (●) cm min^{-1}. Note that σ_y also increases with drawing speed for each n. Vertical lines correspond to the standard deviation, and the solid lines are guides for the eye

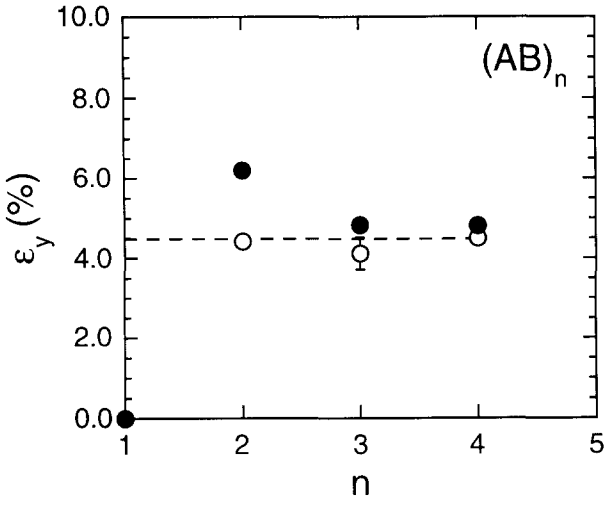

Figure 10 Mean yield elongation (ε_y) as a function of n in these linear $(AB)_n$ copolymers. While σ_y is found to increase with n, ε_y appears to be weakly dependent on n, approaching a constant value of ~4.5% at the two crosshead speeds employed in this work (i.e. 0.5 and 12.7 cm min^{-1}). The symbols are the same as those in *Figure 9*

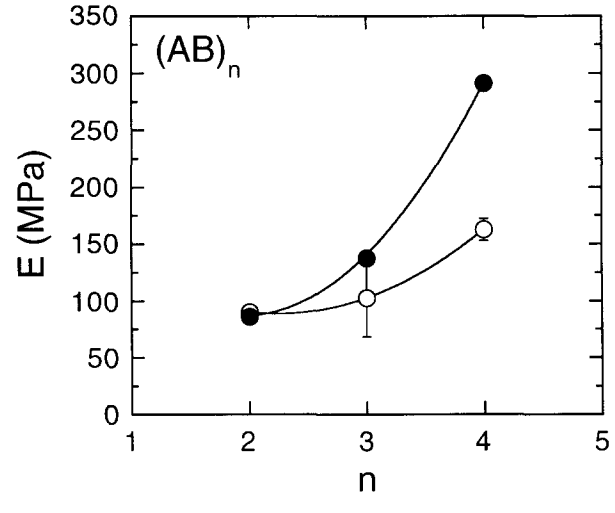

Figure 11 Dependence of the Young's (tensile) modulus (E) on n. The modulus, obtained from the initial σ–ε slope, increases slightly with n at a relatively slow drawing speed (0.5 cm min^{-1}) but then increases dramatically when the copolymers are drawn faster (at 12.7 cm min^{-1}). The behaviour seen here can be attributed to architecture-enhanced microdomain interconnectivity in this series of thermoplastic elastomers. The symbols are the same as those in *Figure 9*, and the solid lines are guides for the eye

copolymers in which M remains constant (and the block lengths decrease with n), the trend evident in *Figure 9* is not attributed to an increase in entanglements which accompany the increase in M ($=nM_{AB}$) in the present copolymer series.

In contrast to $\sigma_y(n)$, values of ε_y measured from curves such as those displayed in *Figure 8* are not very sensitive to either n or the rate of deformation, and maintain a relatively constant value of ~4.5% (*Figure 10*). This relationship is presumed not to be artifactual, since similar results are again obtained[16] from the complementary series of $(SI)_n$ copolymers. Another mechanical property derived from the σ–ε curves in *Figure 8* is the Young's (tensile) modulus, which, assuming constant specimen volume (and a Poisson ratio of 0.5), is determined from the initial slope of σ *versus* ε in the limit of linear (elastic) tensile deformation. From *Figure 11*, the $E(n)$ with $n>1$ are observed to increase slightly with n at the slow crosshead speed and then increase more dramatically with n as the copolymers are drawn faster. This behaviour is consistent with that of $\sigma_y(n)$ described above. It is of interest to note here that, in SIS triblock copolymers, E tends to be independent of the middle isoprene block length but dependent on composition, increasing with the styrene content. In the present work, the composition remains nearly constant, and yet E is found to depend on n. While the preliminary efforts shown in *Figures 8–11* demonstrate that the tensile properties of $(AB)_n$ multiblock copolymers are dependent on n, forthcoming studies will address these architecture–property relationships in other modes of deformation (e.g. dynamic oscillatory shear).

Blend properties. When strongly segregated diblock copolymers are blended with a relatively small quantity of one of the parent homopolymers or a homopolymer that is compatible with either block, a single microphase-separated morphology is normally produced, provided that the molecular weight of the added homopolymer is less than that of the solubilizing block[50–54]. In addition, Hashimoto *et al.*[55] have recently demonstrated that a physical blend of two diblock copolymers tends to be miscible at all compositions, yielding a single morphology, when the ratio of molecular weights is less than 5:1. These characteristics of blends consisting of at least one diblock copolymer are not shared by multiblock copolymers. While the results of some $(AB)_n$ blending studies are presented elsewhere[18,56], we provide some important conclusions here for the sake of completeness.

Binary blends produced with these $(SI)'_n$ copolymers and 6500 g mol^{-1} hPS tend to be macrophase-separated, even though the homopolymer molecular weight is less than half that of a single styrene block in these materials. This observation has been attributed to the highly interconnected microdomains arising from the multiblock architecture. In addition, blends of a symmetric diblock copolymer (with 60 000 g mol^{-1} blocks) and $(SI)_4$ are also only partially miscible. In this case, the molecular weights are identical, and the ratio of block lengths is 4:1. These examples are meant to illustrate that linear diblock copolymers (with $n=1$) and linear multiblock copolymers possess remarkably different blending behaviour, with the latter preferring to self-assemble and exclude an added solute. Consequently, their compatibilizing attributes are also expected[57] to differ.

CONCLUSIONS

The microstructural characteristics and macroscopic properties of linear $(AB)_n$ copolymers ($1 \leqslant n \leqslant 4$) possessing nearly equal block lengths have been studied in an effort to identify key architecture–morphology–property relationships. All four materials are microphase-separated at their upper T_g and exhibit a lamellar morphology in which the microdomain periodicity decreases with n. This reduction in periodicity, observed in TEM micrographs and inferred from SAXS profiles, is predicted by existing theoretical formalisms and indicates that the degree of phase mixing increases with n, in qualitative agreement with d.s.c. measurements of T_g^S. While the thermodynamic driving force favouring microphase separation apparently decreases with n in this series, tensile properties

such as the yield stress and elastic modulus have been found to increase with n, suggesting that microdomain interconnectivity enhances copolymer toughness. Results presented here clearly indicate that microphase-separated linear multiblock copolymers behave quite differently than their diblock analogues and that further study of these materials is required to elucidate the role of the middle blocks on morphology and property development.

ACKNOWLEDGEMENTS

Part of this work has been supported through a start-up grant from the NCSU College of Engineering. Partial support from a Faculty Research and Professional Development Grant (NCSU) is also gratefully acknowledged. We thank Mr M. A. Burchfield (P&G) and Mr J. H. Laurer (NCSU) for their assistance in sample preparation and data reduction.

REFERENCES

1 Leibler, L. *Macromolecules* 1980, **13**, 1602
2 Fredrickson, G. H. and Helfand, E. *J. Chem. Phys.* 1987, **87**, 697
3 Larson, R. G. *J. Chem. Phys.* 1992, **96**, 7904
4 Gehlsen, M. D., Almdal, K. and Bates, F. S. *Macromolecules* 1992, **25**, 939
5 Sakurai, S., Sakamoto, J., Shibayama, M. and Nomura, S. *Macromolecules* 1993, **26**, 3351
6 Chaumont, P., Beinert, G., Herz, J. and Rempp, P. *Polymer* 1981, **22**, 663
7 Ogata, S., Kakimoto, M. and Imai, Y. *Macromolecules* 1985, **18**, 851
8 Ogata, S., Maeda, H., Kakimoto, M. and Imai, Y. *J. Appl. Polym. Sci.* 1987, **33**, 775
9 Arnold, C. A., Summers, J. D., Chen, Y. P., Bott, R. H., Chen, D. and McGrath, J. E. *Polymer* 1989, **30**, 986
10 Feng, D., Wilkes, G. L. and Crivello, J. V. *Polymer* 1989, **30**, 1800
11 Samseth, J., Mortensen, K., Burns, J. L. and Spontak, R. J. *J. Appl. Polym. Sci.* 1992, **44**, 1245
12 Patel, N. M., Dwight, D. W., Hedrick, J. L., Webster, D. C. and McGrath, J. E. *Macromolecules* 1988, **21**, 2689
13 Dwight, D. W., McGrath, J. E., Riffle, J. S., Smith, S. D. and York, G. A. *J. Electron Spectrosc. Relat. Phenom.* 1990, **52**, 457
14 Spontak, R. J., Smith, S. D., Satkowski, M. M., Ashraf, A. and Zielinski, J. M. in 'Polymer Solutions, Blends, and Interfaces' (Eds I. Noda and D. N. Rubingh), Elsevier, Amsterdam, 1992, pp. 65–88
15 Smith, S. D., Spontak, R. J., Satkowski, M. M., Ashraf, A. and Lin, J. S. *Phys. Rev. B* 1993, **47**, 14555
16 Spontak, R. J., Smith, S. D., Satkowski, M. M., Ashraf, A., Heape, A. K. and Lin, J. S. *Macromolecules* to be submitted
17 Spontak, R. J., Zielinski, J. M. and Lipscomb, G. G. *Macromolecules* 1992, **25**, 6270
18 Spontak, R. J., Smith, S. D. and Agard, D. A. in 'Proc. 51st Ann. Meet. Microsc. Soc. Amer.' (Eds G. W. Bailey and C. L. Rieder), San Francisco Press, San Francisco, 1993, pp. 888–889
19 Widmaier, J. M. and Meyer, G. C. *J. Polym. Sci., Polym. Phys. Edn* 1980, **18**, 2217
20 Hadziioannou, G. and Skoulios, A. *Macromolecules* 1982, **15**, 258
21 Spontak, R. J., Smith, S. D. and Ashraf, A. *Polymer* 1993, **34**, 2233
22 Hashimoto, T., Shibayama, M. and Kawai, H. *Macromolecules* 1983, **16**, 1093
23 Sakurai, S., Momii, T., Taie, K., Shibayama, M., Nomura, S. and Hashimoto, T. *Macromolecules* 1993, **26**, 485
24 Albalak, R. J. and Thomas, E. L. *J. Polym. Sci., Polym. Phys. Edn* 1993, **31**, 37
25 Winey, K. I., Patel, S. S. and Larson, R. G. *Macromolecules* 1993, **26**, 2542
26 Hashimoto, T., Shibayama, M. and Kawai, H. *Macromolecules* 1980, **13**, 1237
27 Hadziioannou, G. and Skoulios, A. *Macromolecules* 1982, **15**, 267
28 Almdal, K., Rosedale, J. H., Bates, F. S., Wignall, G. D. and Fredrickson, G. H. *Phys. Rev. Lett.* 1990, **65**, 1112
29 Matsushita, Y., Mori, K., Saguchi, R., Nakao, Y., Noda, I. and Nagasawa, M. *Macromolecules* 1990, **23**, 4313
30 Krause, S. *J. Polym. Sci. A2* 1969, **7**, 249
31 Benoit, H. and Hadziioannou, G. *Macromolecules* 1988, **21**, 1449
32 Kavassalis, T. A. and Whitmore, M. D. *Macromolecules* 1991, **24**, 5340
33 Hong, K. M. and Noolandi, J. *Macromolecules* 1981, **14**, 727
34 Meier, D. J. in 'Thermoplastic Elastomers: a Comprehensive Review' (Eds N. R. Legge, G. Holden and H. E. Schroeder), Hanser, New York, 1987, Ch. 11
35 Henderson, C. P. and Williams, M. C. *J. Polym. Sci., Polym. Phys. Edn* 1985, **23**, 1001
36 Zielinski, J. M. and Spontak, R. J. *Macromolecules* 1992, **25**, 653
37 Semenov, A. V. *Sov. Phys.-JETP (Engl. Transl.)* 1985, **61**, 733
38 Zhulina, E. B. and Halperin, A. *Macromolecules* 1992, **25**, 5730
39 Marko, J. F. *Macromolecules* 1993, **26**, 1442
40 Kane, L. and Spontak, R. J. *Macromolecules* 1994, **27**, 1267
41 Spontak, R. J., Jones, R. L. and Kane, L. *Chem. Eng. Sci.* submitted
42 Helfand, E. and Wassermann, Z. R. *Macromolecules* 1976, **9**, 879
43 Noda, I., Smith, S. D., Dowrey, A. E., Grothaus, J. T. and Marcott, C. *Mater. Res. Soc. Symp. Proc.* 1990, **171**, 117
44 Lu, X. and Jiang, B. *Polymer* 1991, **32**, 471
45 Granger, A. T., Krause, S. and Fetters, L. J. *Macromolecules* 1987, **20**, 1421
46 Diamant, J., Soong, J. S. and Williams, M. C. in 'Contemporary Topics in Polymer Science' (Eds W. J. Bailey and T. Tsurata), Vol. 4, Plenum, New York, 1984, pp. 599–627
47 Henderson, C. P. and Williams, M. C. *Polymer* 1985, **26**, 2026
48 Stöppelmann, G., Gronski, W. and Blume, A. *Polymer* 1990, **31**, 1839
49 Bard, J. K. and Chung, C. I. in 'Thermoplastic Elastomers: a Comprehensive Review' (Eds N. R. Legge, G. Holden and H. E. Schroeder), Hanser, New York, 1987, Sect. 12.1
50 Hashimoto, T., Tanaka, H. and Hasegawa, H. *Macromolecules* 1990, **23**, 4378
51 Tanaka, H., Hasegawa, H. and Hashimoto, T. *Macromolecules* 1991, **24**, 240
52 Winey, K. I., Thomas, E. L. and Fetters, L. J. *Macromolecules* 1991, **24**, 6182
53 Winey, K. I., Thomas, E. L. and Fetters, L. J. *J. Chem. Phys.* 1991, **95**, 9367
54 Spontak, R. J., Smith, S. D. and Ashraf, A. *Macromolecules* 1993, **26**, 956
55 Hashimoto, T., Yamasaki, K., Koizumi, S. and Hasegawa, H. *Macromolecules* 1993, **26**, 2895
56 Spontak, R. J., Smith, S. D. and Ashraf, A. *Macromolecules* 1993, **26**, 5118
57 Balazs, A., Siemasko, C. P. and Lantman, C. W. *J. Chem. Phys.* 1991, **94**, 1653